EXPLAINING CO-SEISMIC STRAINS ON PBO BOREHOLE STRAINMETERS

ANDREW J. BARBOUR, DUNCAN C. AGNEW

EarthScope National Meeting — May, 2011 — Austin, TX

Introduction

We have observed permanent[1] strain offsets occurring at Plate Boundary Observatory (PBO) borehole strainmeters (BSM) as a result of the rapid dynamic-straining from significant earthquakes[2]. Our analyses show these co-seismic offsets are not resultant of pore-fluid pressure changes[3], and cannot be adequately modeled by a point- or distributed-source in an elastic half-space[4]: We observe magnitude discrepancies upwards of 100 times too large, and 20 times too small. Layered models do not improve the fit well enough to account for this apparent anelastic behavior. Consistent trends by station and channel appear absent (Figure 1). There are discrepancies in polarity too: Nearly 3/4 of the observed offsets shown in fig. 1 have the incorrect sign, according to elasticity predictions. Alternative high-sensitivity geodetic observations [i.e. long-baseline laser strainmeters (LSM) and GPS offsets] confirm the lack of agreement between theory and observation.

Assuming the BSM maintains it's high elastic-compliance over all strain rates, these discrepancies suggest the offsets manifest local strain tensor modification by some nearby process, apparently activated or enhanced by rapid strain-rate changes. Our presentation explores the possibility that the combination of tectonic setting and geologic environment of the borehole controls this effect, rather than tectonic strain redistribution and/or pore-fluid pressure perturbation. For example, activation of a nearby joint (with slippage) could theoretically[5] produce enough strain to affect the borehole measurement and remain undetected by other high-resolution instrumentation (i.e. the LSM).

Peak strains, ground velocities, and accelerations

Although the BSMs measure only a horizontal strain tensor, and do not record ambient Earth strain at periods shorter than 1 second[6], we investigate ground motions which produce co-seismic offsets. To do this we compare peak strains from strong earthquakes to peak accelerations and velocities very nearby. In the case of the Anza-cluster instruments, 7/8 boreholes are instrumented with short-period, three-component geophones, sampled

[1] Insofar as the random-walk nature of Earth strain permits such a definition.

[2] cataloged by the National Earthquake Information Center

[3] Observed re-equilibrium timescales for the associated pressure disturbances - at the BSMs - are on the order of days.

[4] Okada, Y. (1992), Internal deformation due to shear and tensile faults in a half-space, *BSSA*, *82*(2), 1018–1040.

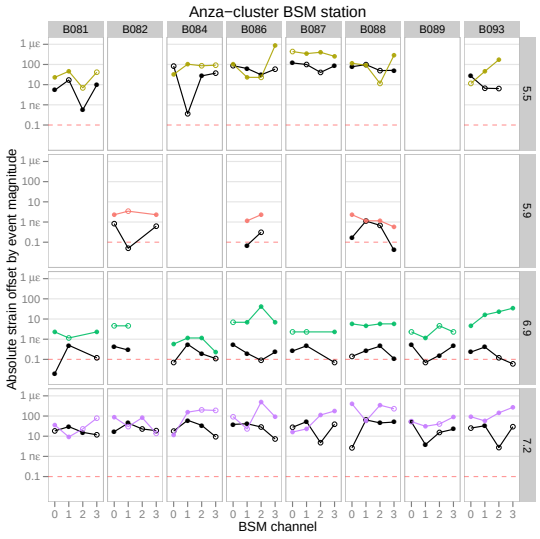

Figure 1: Offsets on Anza-cluster borehole strainmeters (colors) versus model predictions (black) and resolution (dashed). Rows show data for the same earthquake but different stations, with axes representing log-strain; columns show data for the same station but different earthquakes, sorted by channel. Symbols encode polarity. *Predictions are based on moment tensor solutions (NEIC, NCEDC).*

[5] Molnar, P., R. S. Anderson, and S. P. Anderson (2007), Tectonics, fracturing of rock, and erosion, *J. Geophys. Res.*, *112*(F03014).

[6] Barbour, A. J., and D. C. Agnew (2011), Noise Levels on Plate Boundary Observatory Borehole Strainmeters in Southern California, *submitted to Bull. Seismol. Soc. Amer.*.

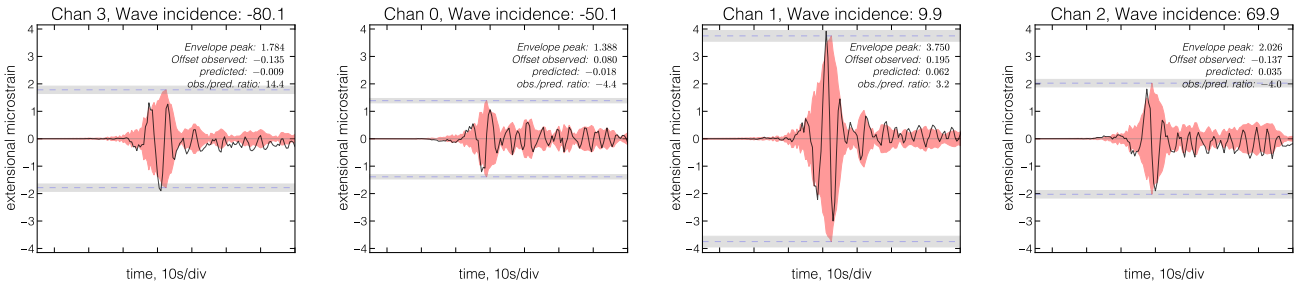

Figure 2: Linearized, high-frequency (periods > 2 sec) strain data before and during the Sierra El Mayor/Cucapá mainshock ($M_w = 7.2$) on April 4, 2010, for all channels at B084 at the Piñon Flat Observatory (PFO); the order from left to right is by increasing wave-incidence angle. The strain envelope, calculated using a Hilbert transform on band-limited data (to remove an artifact introduced by the offset), is shown as a red filled-region plotted ± 0 strain. As is obvious for channel 1, the offset record exceeds the envelope prior to (or very close to) peak strain; this indicates the permanent offset develops rapidly after first arrivals.

at 100 Hz; and three-component strong-motion accelerometers, sampled at 200 Hz. An example of peak strains from the Sierra El Mayor/Cucapá (EMC) mainshock ($M_w = 7.2$) on April 4, 2010 is shown in Figure 2. The data are from B084 at the Piñon Flat Observatory (see Figure 3), located tens of kilometers northeast from the San Jacinto fault; they show clear permanent offsets and large dynamic strains (max. 3.8 microstrain). Offsets do not occur instantaneously at the P-wave arrival but develop very rapidly after the first arrivals. It's unclear whether they develop discretely, or cumulatively over a series of smaller events initiated by the P-wave. We do not observe similar behavior from teleseismic waves, suggesting the offset is unaffected by long-period surface waves, and controlled primarily by high-frequency body waves.

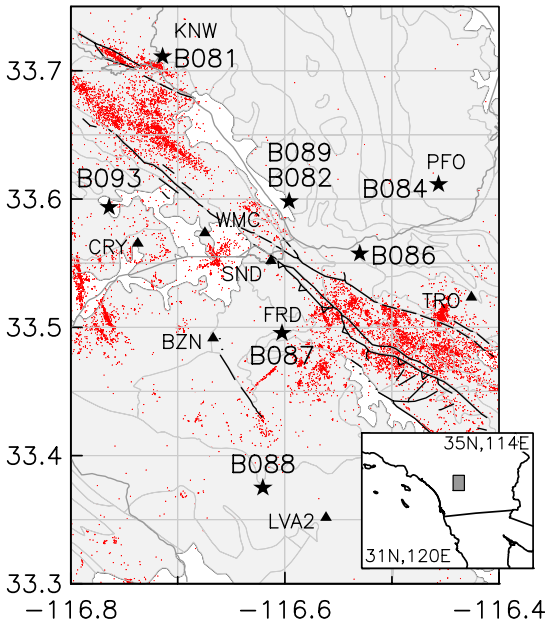

Figure 3: Locations of PBO boreholes (★), Anza broadband seismometers (▲), relocated seismicity (red dot), regions of primarily crystalline surface geology (gray regions), and the San Jacinto fault system (black lines).

Groundtruth

We compare our observations of co-seismic strain with independent geodetic measurements, namely InSAR, LSM, and GPS.

Unfortunately, Synthetic Aperture Radar interferograms (InSAR) are too poorly correlated in the Anza region, have coarse temporal resolution, and significant uncertainty from various non-tectonic sources, making it difficult to analyze very small deformations in this context.

At PFO the borehole strainmeter is colocated with three independent LSM, making direct comparisons of high-resolution strain possible. Such a comparison constrains the lower limit of measurable signal at length scales of hundreds of meters, but they must be scrutinized carefully: Strong shaking has a tendency to cause mis-counting of the interference fringes. In Figure 4 we show data from an earthquake on a transform fault in the Gulf of California

(August 3, 2009; M_w=6.9), during which all three LSMs maintain fringe count. Even on a expanded strain scale, no significant offset shows in the LSM data, while clearly each BSM is offset. The epicenter is 609 km away from PFO along the WGS84 geodesic, whereas the separation between the BSM and LSM is 75 meters or less.

Even with a relatively sparse field of co-seismic GPS displacements and their uncertainties, it is possible to solve for an empirical strain-tensor field[7]. We perform such a computation using the `SSPX` program and offsets from continuous GPS sites in southern California[8]. We calculate the horizontal field, and the associated uncertainties, using a "nearest neighbor" calculation with distance attenuation[9]. Results for the EMC earthquake are shown in Figures 5–8.

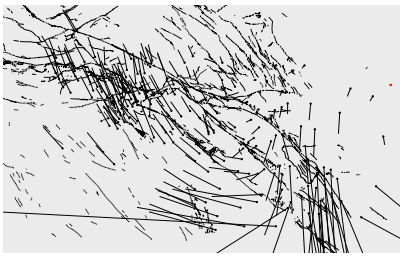

Figure 5: Map of co-seismic displacements (exaggerated) at continuous GPS sites in southern California; secular trends and post-seismic motions are removed.

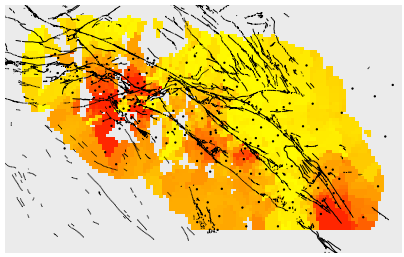

Figure 6: Map of uncertainties in the strain field calculation; linear color scale ranges from BSM instrumental resolution (0.1 nanostrain, yellow) to 100 nanostrain (red).

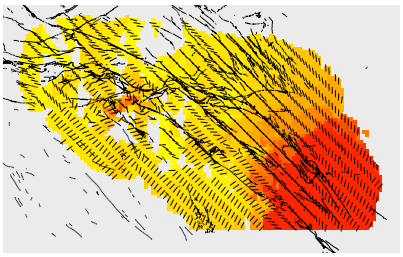

Figure 7: Map of extensional strain with principle directions; linear color scale ranges from BSM instrumental resolution (0.1 nanostrain, yellow) to 1000 nanostrain (red).

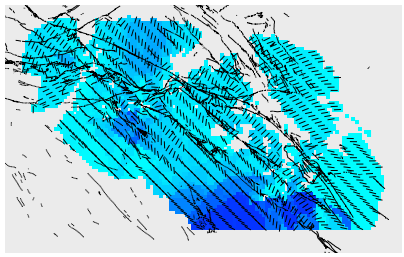

Figure 8: Map of contractional strain, with principle directions; linear color scale ranges from BSM instrumental resolution (-0.1 nanostrain, cyan) to -1000 nanostrain (blue).

The GPS displacements provide valuable upper limits on the magnitude of strain observed over a wide area. At and around the Anza-cluster strainmeters, the GPS solution shows permanent extensional strains of up-to 200 nanostrain and unresolvable contractional offsets; the uncertainty in the solution is at least 20 nanostrain. We compare these groundtruth results in Table 1 for the Anza-region, and the strainmeters installed there.

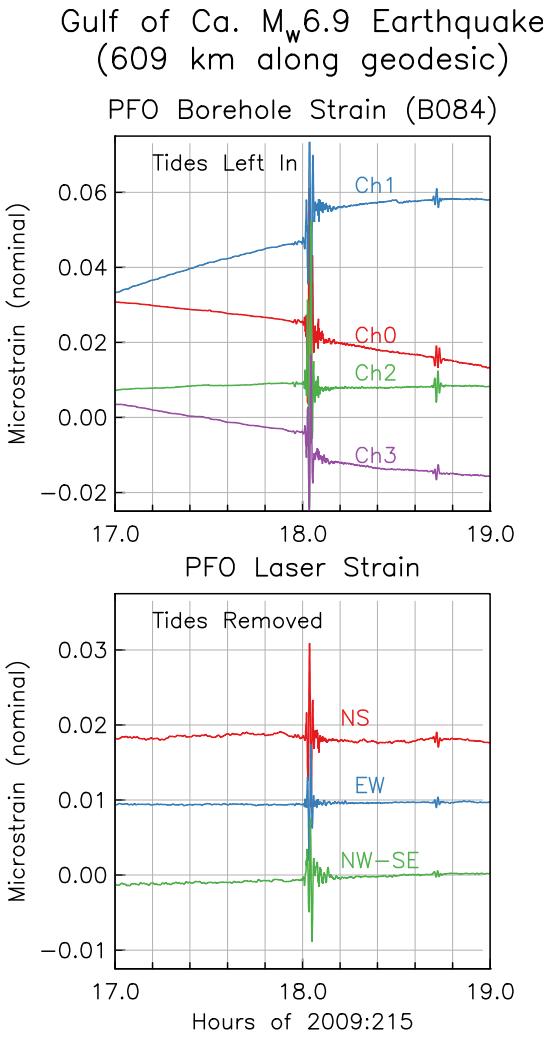

Figure 4: BSM and LSM measurements of the 2009:215 Gulf of California earthquake (M_w = 6.9) at PFO. *Note the vertical scale change.*

[7] Cardozo, N., and R. Allmendinger (2009), SSPX: A program to compute strain from displacement/velocity data, *Computers & Geosciences*, *35*(6), 1343 – 1357.

[8] Secular pre-seismic trends, and post-seismic relaxation are removed (B. Crowell, pers. commun., Jan. 2011)

[9] Weighting follows $\exp(-d^2/2\alpha^2)$, where d is the distance to a nearby station, and α is the attenuation factor (70 km in our calculations).

	Co-seismic offset range in Anza, CA (nanostrain, 10^{-9})			
	extension		contraction	
	lower	upper	lower	upper
Okada solution	15	94	3	70
GPS solution	50 ± 20	200 ± 20	—	—
BSM observed	9	495	13	230
LSM observed	*unavailable*			

Table 1: Ranges of co-seismic extensional and contractional offsets from the EMC mainshock: Theory (Okada), groundtruth (GPS), and observation (BSM). The "—" marker indicates the value is below the resolution of the BSM (0.1 nanostrain). The LSM comparison is unavailable because of mis-counting.

The Borehole Environment

Instruments in the Anza-cluster are located within tens of kilometers of a proposed slip-gap along the main trace of the San Jacinto fault (SJF) — the "Anza gap". The SJF system accommodates a large proportion of the total slip budget in the region by dextral shear, with the San Andreas fault accommodating the remaining portion.

We have performed preliminary analyses of logging data recorded during the drilling process. Software is being developed to identify features in the acoustic televiewer data, which provides information on lithological structure, fracturing, and stress orientation. We present results from two sites northeast of SJF: B082 (Pathfinder Ranch), located in an alluvial basin; and B084, located in granitic pluton (see Fig. 3). Fracture orientations for these boreholes are shown in Figure 9. Fractures identified for site B082 show trends in strike and dip consistent with shearing on the SJF and regional compression, as well as highly-scattered anisotropy observations[10]; fractures at B084 are not preferentially oriented.

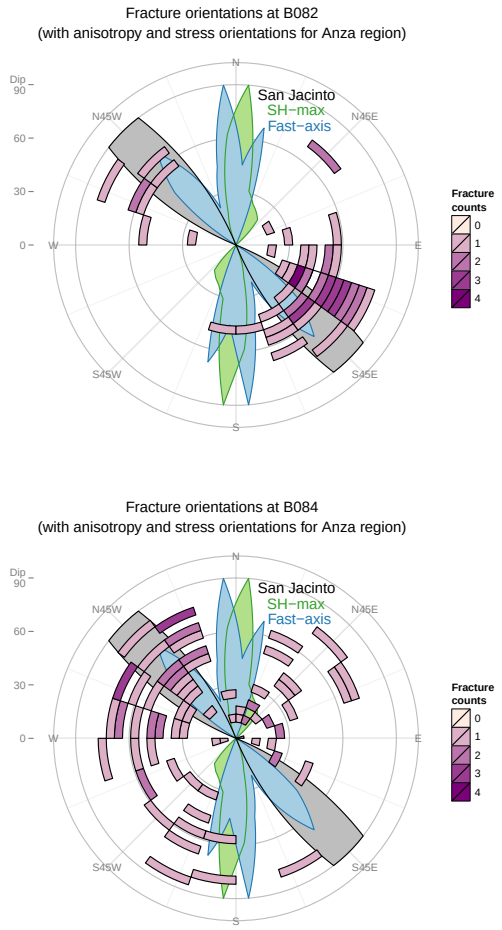

Figure 9: Fracture orientations at B082 (top) and B084, overlain on orientations of the San Jacinto fault, crustal stress (green), and shear-wave splitting fast-axes (blue) in the Anza region.

[10] Yang, Z., A. Sheehan, and P. Shearer (2011), Stress-induced upper crustal anisotropy in southern California, *J. Geophys. Res.*, *116*(B2).